

Can Geologic Factors be Predictive for Distinguishing between Productive and Non-productive Geothermal Wells?

Drew L. Siler, Erick R. Burns, James E. Faulds

¹**U.S. Geological Survey, 345 Middlefield Rd, Menlo Park, California 91025**

²**U.S. Geological Survey, 2130 SW 5th Ave, Portland, Oregon, 97201**

³**Nevada Bureau of Mines and Geology, University of Nevada, Reno, NV 89557**

Keywords

Geology, faults, Brady, stratigraphy, exploration, stress-strain, productivity

ABSTRACT

Geologic data are examined in order to evaluate whether certain geologic characteristics occur in higher abundance or higher magnitude along geothermal production wells relative to non-productive wells. A 3D geologic map, a 3D stress model, and fault-slip modeling are used to estimate fourteen different geologic factors that are hypothesized to control or be correlated with well productivity. The geologic factors are; heat, fault-damage zone thickness, distance from active faults, fault intersection/termination density, fault curvature, slip tendency of faults, dilation tendency of faults, dilation resulting from modeled fault slip, normal stress reduction resulting from modeled fault slip, Coulomb shear stress increase resulting from modeled fault slip, the summed thickness of ‘favorable’ lithologies within a borehole, the summed thickness of fault damage zones in favorable lithologies within a borehole, the distance along the borehole to the nearest geologic contact, and the thickness of individual stratigraphic units. These geologic factors are quantified along fifty wells at Brady geothermal system, including twelve production wells and thirty-one non-productive wells. Results indicate that geologic factors such as stress changes associated with faulting, nearness to and thickness of fault zones, distance from geologic contacts, and heat occur in higher magnitude or higher abundance along production wells relative to non-productive wells. These geologic factors may play an important role, controlling the locations and distribution of fluid circulation in geothermal fields.

1. Introduction

Free convection and/or precipitation-driven recharge drive fluid circulation through permeable pathways in the crust. In many types of geologic systems, primary permeability is preferentially horizontal, associated with alternating high and low permeability in the stratigraphic succession. Zones of fracture permeability along faults (secondary permeability) serve as conduits for both vertical and horizontal flow, and also barriers to horizontal flow. In hydrothermal systems, hot fluids upwell through the crust towards the shallow subsurface through zones of very restricted areal extent (focused discharge). Not all faults, however, are sufficiently permeable to transmit fluids. The capacity of a fault to transmit fluids varies depending on local conditions within the fault segment. Even if a fault segment can transmit fluid, the fault must be connected to a network of permeable zones to generate a connected pathway for fluids to circulate.

Fracture flow can be conceptualized as a branching network with few through-going conduits. Many branches lead to dead ends, ultimately resulting in a flow system that connects with a larger volume of rock relative to the spatially restricted through-going channels that transmit most of the flow. A geothermal production well may intersect many branches (i.e., through-going or dead-end), with the well forming a new flowing pathway to land surface. The above explains why many geothermal production wells produce from intervals that are confined to a few meters or less along the well path (based on Nevada Division of Minerals, publicly available data). Understanding the local geologic controls on the locations, extent, spatial distribution, and connectivity of the vertical and horizontal ‘branches’ of the flow system is crucial to understanding of a geothermal flow system. In this study we focus on the Brady geothermal area and examine fourteen different geologic factors that are hypothesized to control the distribution of permeability and fluid circulation. The geologic factors are well-constrained by extensive published work at Brady. The factors are compared along fifty existing wells: five highly productive wells, seven moderately productive wells, seven condensate reinjection wells, and thirty-one wells that were not significantly productive (hereafter called, non-productive wells).

2. Background

The Brady geothermal area is the focus for our comparison between the geologic characteristics of productive and non-productive geothermal wells. The Brady area is well-suited for this study, with well-characterized subsurface geology and fifty wells that are variably productive. The Brady area is located in northwestern Nevada, ~90 km northeast of Reno, Nevada. In addition to the fifty wells utilized in this study, there are dozens of other wells, including shallow temperature gradient wells, that have been drilled since exploration began in the 1950s. The permeable pathways of the geothermal system pass through the Brady fault zone, a north-northeast-striking, northwest dipping normal fault zone (Figure 1). The most recent displacement along the Brady fault zone is younger than ~15,500 yrs (Wesnousky et al., 2005). The geothermal field and associated hydrothermal features occur along ~2.5 km of strike-length. Hydrothermal features include active fumaroles, silica sinter, calcium carbonate tufa, silicified sediments, and warm ground (Kratt et al., 2006; Lechler and Coolbaugh, 2007; Faulds et al., 2010a; Faulds et al., 2010b; Faulds et al., 2017). Within the ~2.5 km zone of hydrothermal features, there is a ~1 km-wide ~2 km long (across-strike by along-strike) left step-over in the Brady fault zone. This area hosts the highest subsurface temperatures and all of the production

wells (Faulds et al., 2010b; Faulds et al., 2010a; Shevenell et al., 2012; Siler et al., 2015; Ali et al., 2016; Queen et al., 2016; Faulds et al., 2017). The production well field at Brady (Figure 1) supplies 26.1 MWe and ~7 MWth to a power station and a direct-use vegetable drying facility, respectively.

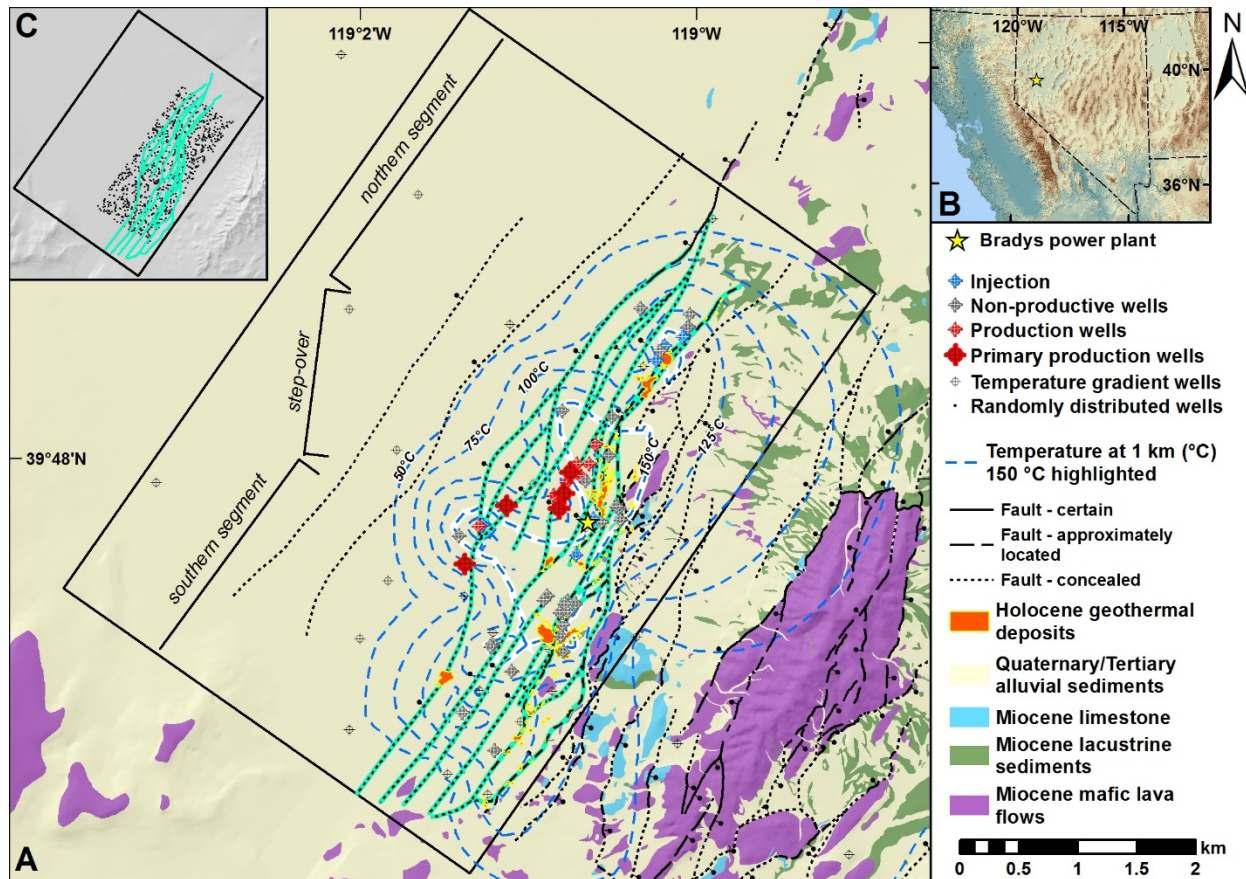


Figure 1. Geologic map of the Brady area (simplified after Faulds et al., 2017). The Brady fault zone is shown highlighted in green. The fifty wells used in this study are shown. C) shows the spatial distribution of the 1000 randomly distributed synthetic wells used in the analysis.

3. Methods

The 3D geometries of faults and geologic contacts from a 3D geologic map are the baseline data used to evaluate fourteen different geologic-based factors that are hypothesized to affect the productivity or non-productivity of geothermal wells. A 3D geologic map (Siler and Faulds, 2013; Siler et al., 2016) building upon published 3D analyses at Brady (Jolie et al., 2012; Jolie et al., 2015) and incorporating additional data and additional stratigraphic and structural complexity relative to the earlier efforts was used in this study (Figure 2). The 3D map was constructed using established methods (e.g., Moeck et al., 2009a; Moeck et al., 2009b; Siler et al., 2019). The 3D map incorporates interpretation of four 2D seismic reflection profiles, down-hole lithologic

data based on analyses of drill cuttings and core from twenty-four wells, and 1:12,000 scale geologic mapping and associated geologic cross-sections (Faulds et al., 2010b; Faulds et al., 2010a; Jolie et al., 2012; Siler and Faulds, 2013; Jolie et al., 2015; Queen et al., 2016; Siler et al., 2016; Faulds et al., 2017). Published 3D inversion of gravity data, which incorporates constraints on rock densities measured throughout the geologic section from core and outcrop samples confirms that the geologic unit thicknesses and distributions in the 3D geologic map of the Brady area are consistent with the gravity measurements (Witter et al., 2016). In the following analysis we consider the occurrence and distribution of fourteen geologic factors constrained by 3D geologic map along fifty geothermal wells in the Brady area (Figures 1 and 2).

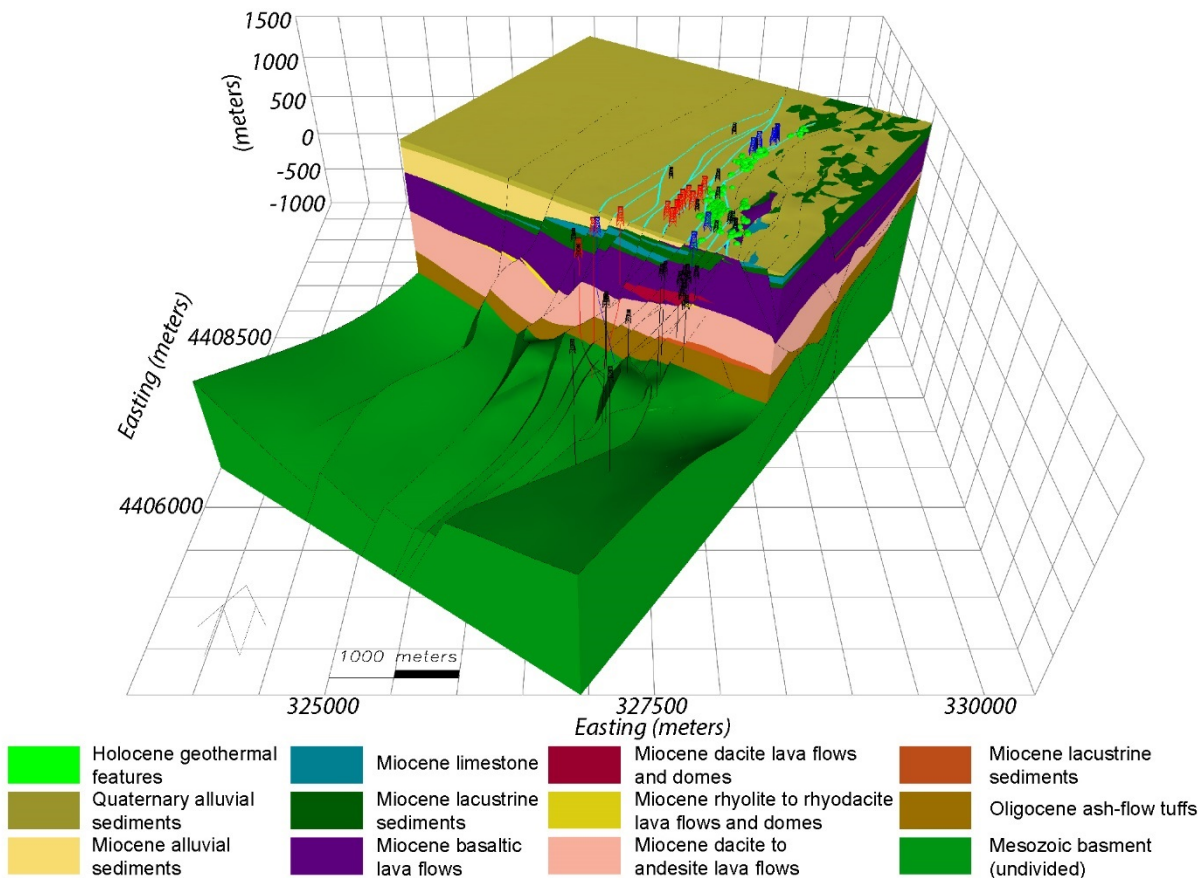


Figure 2. 3D geologic map (Siler and Faulds, 2013; Siler et al., 2016; Witter et al., 2016) of the Brady geothermal field used to constrain the fault and stratigraphic factors in this study. The fifty wells used in the study are shown, well color codes are the same as Figure 1.

Geothermal Well Productivity Data

Twelve of the fifty wells examined in this study were utilized for geothermal production in the Brady geothermal field between 1992 and 2013 (based on publicly available data, Nevada Division of Minerals). Data more recent than 2013 were not readily available and therefore were not utilized in this study. Of the twelve production wells, five wells were used for production for

greater than 60% of the time since each well was originally brought online. In other words, these five wells have been supplying fluid to the power station for the majority of their life-spans. We therefore considered them ‘primary production wells’ in this study. The other seven production wells were used for production for significant periods of time between 1992 and 2013 but have not been used for production for the majority of their life-spans. For our analyses we consider these other seven wells simply as ‘production wells.’ The locations of the production wells and primary production wells are shown on Figures 1 and 2.

Seven of the fifty wells used in this study have been used for injection of discharge from the Brady power station between 1992 and 2013. An additional four wells located in a neighboring basin ~6 km south of the geothermal field have also been used for injection during this time period. This distal basin is not hydrologically connected to the Brady geothermal field. Therefore, we only consider the seven injection wells that are located within the Brady geothermal field in the following analyses. The locations of the injection wells are shown on Figures 1 and 2.

The thirty-one remaining wells used in this study have never been used for injection or production. We assume that these thirty-one wells have sub-commercial temperatures and/or fluid flow volumes and rates. We do not know what each of these thirty-one wells was drilled for. It is possible that several of these wells were never intended to be used as geothermal production wells, if they were drilled as stratigraphic test wells, for instance. However, we suggest that if any of these wells had encountered significant hot in flow, regardless of their original purpose, it is likely that it would have been re-drilled as a geothermal production well at some point during development of the field. These thirty-one wells are therefore assumed to be ‘non-productive wells’ in the following analysis. The locations of the non-productive geothermal wells are shown on Figures 1 and 2.

A synthetic dataset of 1000 vertical wells with random spatial distribution along the Brady fault zone and random depths (between ~500 and 1800 m, the depth range of the twelve production wells) is also used in the following analysis. Use of a high density of synthetic wells allows a comparison between productive wells and the geologic conditions that exist throughout the domain of interest. Mathematically, this allows evaluation of the null hypotheses, which answers the question: are conditions in productive wells distinguishable from ‘background’ conditions? The distribution of the 1000 synthetic wells is shown in Figure 1C.

Conceptual model of geothermal system permeability

Permeability in a hydrothermal system discharge zone is conceptualized as a branching network of variably discontinuous vertical and horizontal fractures associated with both secondary, fracture permeability and primary lithologic permeability. There are one or more connected flow paths that allow the vertical movement of fluids from depth, and therefore effective and efficient transport of heat. Regional stress conditions and local geological characteristics may foster open vertical fractures in localized regions, but due to geologic heterogeneity and variable stress accommodation across stratigraphic layers, single chimneys cutting continuously through the stratigraphic section are not likely to exist. Instead, vertical fractures are offset between layers, and either primary or secondary permeability must connect these vertical fractures to create the complete and fully connected flow path. This pattern results in many dead-end flow paths. Though individual flow paths are randomly distributed and arranged, in areas of favorable stress

and geologic conditions the density of fractures (potential flow paths) is higher, and therefore the likelihood of connectivity of a large volume is higher.

The ideal production well intersects one or more sub-vertical flow paths that are fed by flow through a network of branches throughout the section. Non-productive wells probably intersect branches and/or dead-ends flow paths that are poorly connected with the main vertical flow paths, resulting in sub-commercial productivity. By evaluating the geological, structural, and stress factors that control or correlate with vertical and horizontal permeability, we hope to constrain the conditions that may lead to the development of sub-vertical flow paths that are fed by a large connected fracture network, and therefore increase the ability to predict the locations of these features.

Measures that are postulated to be correlated to productivity

Based on the conceptual model of geothermal system permeability and heat flow, we hypothesize that each of the following measurable factors affect the productivity vs. non-productivity of a geothermal well. They may generally be broken into factors related to heat flow, structure, stress-strain conditions, and lithology.

Heat Flow

- **Heat:** Because heat conducts away from zones of advective heat delivery, higher temperatures are correlated to regions where a connected network of fractures is transporting a hydrothermal fluid, regardless of whether or not the borehole intersects the advective zone. Therefore, higher temperatures indicate closer proximity to permeable pathways. For locations where temperature has not been directly measured, a 3D temperature model was constructed, using equilibrated temperature logs from thirty-nine deep geothermal wells and seventy-nine shallow temperature gradient wells (Shevenell et al., 2012). The temperature along each of the fifty wells used in our analysis is integrated and divided by the well length, resulting in one integrated heat value per well. Higher heat values are hypothesized to correlate with productive wells relative to non-productive wells.

Structural factors

- **Damage zone thickness:** We hypothesize that densely fractured regions in fault damage zones have a higher likelihood of resulting in longer and connected flow paths. Therefore, the probability of intersecting a fracture connected to the hydrothermal system increases with increasing number and/or total thickness of fault damage zones intersected by the well. For each 3D fault plane, a 30 m wide zone representing the fault damage zone in which fracturing is accentuated relative to surrounding intact rock is generated. The integrated thickness of damage zone along each well is divided by the well path length, resulting in one integrated damage zone thickness value for each well. A greater total thickness of fault damage zone per well length is expected to correlate with productive wells relative to non-productive wells.
- **Distance from faults:** Mapped faults are our best indicator of the locations where vertical conduits connected to a large volume of fracture may occur in the subsurface, so we

hypothesize that wells that are near 3D mapped faults are likely to be connected to flow paths that may host hydrothermal fluids. Fault and fracture density generally decreases with increasing distance from a fault (Cowie and Scholz, 1992; Scholz et al., 1993). The distance from each 3D fault plane is calculated, and the distance from faults along each well is integrated and divided by the well length. Lower values indicate wells that pass near to many faults and are hypothesized to correlate with productive wells relative to non-productive wells.

- 3D density of fault intersections and fault terminations: The intersections between steeply dipping faults are manifest as steeply plunging zones of high fracture density. These areas may represent sub-vertical conduits that are connected to large fracture volumes. Tectonic stresses are concentrated at structural discontinuities like fault intersections and fault terminations (Pollard and Aydin, 1988; Rubin and Pollard, 1988; Scholz et al., 1993; Sibson, 1994; Peacock et al., 2000; Sanderson and Zhang, 2004; Fossen and Rotevatn, 2016; Siler et al., 2018). These locations are likely to host higher densities of secondary faults and fractures relative to areas distal to discontinuities. We hypothesize that wells intersecting more dense areas of fault intersections and terminations are more likely to be productive, whereas wells intersecting less dense areas of fault intersections are likely to be non-productive. The 3D fault intersection/termination density is calculated throughout the geothermal field and the intersection/termination density along each well is integrated and divided by well length. Higher values of intersection/termination density are hypothesized to correlate with productive wells relative to non-productive wells.
- Curvature of faults: Similar to fault intersections and terminations, tectonic stresses are concentrated at highly curved areas of faults (Sibson, 1994). Along-strike curvature may result in the formation of sub-vertical zones of permeability, whereas down-dip curvature may result in sub-horizontal permeability, both of which could be connected to a large fracture network. The most highly curved segments of faults therefore are expected to be places with accentuated secondary faulting and fracturing and increase likelihood for fracture connectivity. We hypothesize that wells intersecting the most highly curved segments of faults are more likely to be productive relative to wells intersecting planar fault segments. The angular change in strike and dip (i.e., curvature) along each 3D plane is calculated. The maximum curvature for faults intersected by each well is used because the most highly curved faults are expected to be associated with the highest fracture density. Higher values for curvature are hypothesized to correlate with productive wells relative to non-productive wells.

Stress-strain factors

- Slip tendency on 3D faults: Faults and fractures that have a high resolved shear stress under modern stress conditions are likely to be critically stressed (i.e., expected to slip given some cohesion and pore pressure) and conduct fluids relative to faults with low shear stress (Barton et al., 1995; Zoback and Townend, 2001) and that such faults may connect to large volumes of connected fractures. We hypothesize that wells intersecting faults that are well oriented to have high resolved shear stresses are more likely to be productive relative to wells intersecting less well oriented faults. A normal faulting 3D

stress model (Jolie et al., 2015) with the minimum horizontal stress oriented along azimuth 097 is used. Slip tendency (the ratio of the resolved shear stress to resolved normal stress on a fault) is calculated using methods of (Morris et al., 1996). The maximum slip tendency for faults intersected by each well is used because the highest shear stress faults are expected to slip, resulting in open fractures. Higher values of slip tendency are hypothesized to correlate with productive wells relative to non-productive wells.

- Dilation tendency on 3D faults: Faults and fractures that are well-oriented for dilation under modern stress conditions are likely to be associated with open fractures and more likely to connect a large, branching fault network. We hypothesize that wells intersecting faults that are well oriented for dilation are more likely to be productive relative to wells intersecting faults that are less well oriented for dilation. The same stress model that is used to calculate slip tendency (Jolie et al., 2015) is used to calculate dilation tendency, which is the ratio of stresses acting normal to a fault. Dilation tendency is calculated using methods of (Ferrill et al., 1999). The maximum dilation tendency for faults intersected by each well is used because faults with the highest dilation tendency are expected contain in open fractures. Higher values for dilation tendency are hypothesized to correlate with productive wells relative to non-productive wells.
- Dilation resulting from fault slip: Dilatational fault segments may provide sub-vertical pathways linking many sub-horizontal and sub-vertical zones of permeability in a flow system. Structural discontinuities, like the step-over in the Brady fault zone, focus tectonic stress changes when fault slip occurs. Published slip modeling on the Brady fault zone indicates that when slip occurs dilation is focused on faults within and around the step-over, whereas areas distal to the step over experience shortening (Siler et al., 2016). We hypothesize that wells located in areas that experience high dilation as a result of fault slip will be associated with a large volume of open and connected fractures and therefore more likely to be productive relative to wells in areas that experience less dilation or shortening. The modeled dilation/shortening on optimally oriented faults at geothermal reservoir depth (1000 m) resulting from 1 m normal slip (results from Siler et al., 2016) is calculated for each well. Higher values of dilation are hypothesized to correlate with productive wells relative to non-productive wells.
- Normal stress change resulting from fault slip: Faults and fractures subject to relatively low normal stress are likely to slip, generating and/or maintaining permeability along that fault or fracture. These faults and fractures may become important members of an interconnected fracture network. Slip modeling on the Brady fault zone indicates that when slip occurs reduction in normal stresses on faults occur within and around the Brady step-over, whereas faults distal to the stepover experience an increase in normal stress (Siler et al., 2016). We hypothesize that wells located in areas that experience higher reduction in normal stress as a result of fault slip are likely to be associated with elevated secondary faulting and fracturing and open fractures and therefore more likely to be productive relative to wells in areas that experience a smaller reduction or an increase in normal stress. The modeled normal stress change on optimally oriented faults at geothermal reservoir depth (1000 m) resulting from 1 m normal slip (results from Siler et

al., 2016) is calculated for each well. Higher values indicate normal stress reduction (i.e., unclamping of faults) and are hypothesized to correlate with productive wells relative to non-productive wells.

- Coulomb shear stress increase resulting from fault slip: Similar to dilation and normal stress faults and fractures subject to relatively high Coulomb shear stress are likely to slip, generating and/or maintaining permeability along that fault or fracture. Slip modeling indicates that when slip occurs on the Brady fault zone, Coulomb shear stresses increase on faults within and around the Brady step-over and decrease on faults distal to the stepover (Siler et al., 2016). This zone of stress increase may represent an area with a relatively dense network of interconnected faults and fractures. We hypothesize that wells in these areas are more likely to be productive relative to wells in areas that experience a smaller increase or a decrease in Coulomb shear stress. The modeled Coulomb shear stress change on optimally oriented faults at geothermal reservoir depth (1000 m) resulting from 1 m normal slip (Siler et al., 2016) is calculated for each well. Higher values of Coulomb shear stress change are hypothesized to correlate with productive wells relative to non-productive wells.

Lithologic factors

- Thickness of favorable lithologies: Certain lithologic units have relatively high primary permeability or may be prone to large aperture fractures where faulted. In both cases, that lithologic unit may constitute a significant component of an interconnected fracture network. Lithologic logs show that productive intervals along the twelve Brady production wells occur in certain lithologic units and not in others. In the Brady section, certain shallow volcanic units as well as certain deep volcanic and metamorphic units host productive zones, whereas other units (though the entire section is extensively faulted) do not host any productive zones (Siler et al., 2016). We hypothesize that certain units are relatively strong, coherent lithologies and that, where faulted, can support large aperture fractures, whereas other (perhaps weaker or less coherent) lithologies deform more diffusely and are not prone to large aperture fractures. It is also possible that the primary permeability in these units is an important component of an interconnected fluid flow system. For each well, the integrated thickness of lithologic units known to host fluid flow is divided by the well path length. A greater thickness of ‘favorable’ lithology per well length is expected to correlate with productive wells relative to non-productive wells.
- Damage zone thickness in favorable lithologies: Similar to the above, if certain lithologies are likely to host large aperture fractures, then faults cutting through these units are likely to form permeable damage zones that may connect to a fracture network. We hypothesize that wells intersecting more faults cutting those favorable lithologic units are more likely to be productive than wells intersecting fewer faults in those favorable lithologies. For each well, the integrated thickness of fault damage zone (defined above) contained within the favorable lithologic units that known to host fluid flow is divided by the well path length. A greater thickness of faulted ‘favorable’ lithology per well length is expected to correlate with productive wells relative to non-productive wells.

- Distance from geologic contact: Where faulted, the discontinuities between lithologic units (geologic contacts) may be associated elevated porosity and permeability relative to the interiors of those lithologic units. Alternatively, the combination of existing sub-horizontal permeability along geologic contacts with sub-vertical fault related permeability may result in significant fracture connectivity along geologic contacts. In either event, we hypothesize, that wells that intersect near to many geologic contacts are more likely to be productive relative to wells that intersect areas that are farther from geologic contacts. The distance from each geologic contact is calculated, and the distance from geologic contacts along each well is integrated and divided by the well length. Lower distances from geologic contacts indicate wells that pass near to many contacts and are hypothesized to correlate with productive wells relative to non-productive wells.
- Thickness of lithologic units: Faults cutting through relatively thick lithologic sections may be better suited to focus strain on a few (perhaps large aperture) fractures and therefore connect to a fracture network, more so than faults cutting through a series of thin units. We hypothesize that wells intersecting thick stratigraphic units are more likely to be productive relative to wells intersecting thinner units. The median thickness of each lithologic unit intersected by each well is calculated. We expect higher values, wells intersecting thicker lithologic units, to correlate with productive wells relative to non-productive wells.

4. Results

Sections of production wells where all the geologic factors examined are relatively high are correlated with fractures that produce geothermal fluids. Figures 3A and 3B illustrate the variation in ten of the geologic factors presented above along two of the primary production wells at Brady. The left panel of Figures 3A and 3B shows the variation in each factor along the two wells. Note that the y-axis scale (measured depth in meters) on the Figures 3A and 3B are different, well 1 is ~1800 m deep whereas well 2 is ~550 m deep. Only ten of the fourteen factors are plotted on Figure 3. Dilation, Coulomb shear stress, and normal stress are calculated as one value per well, rather than variable with depth, and therefore are not plotted. Additionally, damage zone thickness in favorable lithology is not plotted, since it is a combination of two factors that are plotted (faults and favorable lithology).

All values shown are normalized to fall between 0 to 1 for ease of visual comparison. Positive values (to the right) are hypothesized to positively correlate with well productivity and zero values (to the left) hypothesized to be anti-correlative to well productivity. Distance to faults and distance to geologic contacts are plotted as inverse (fault or contact nearness, rather than distance) so that all of factors hypothesized to correlate with productive wells increase in value. The red lines in the middle panel of Figures 3A and 3B show a composite score along the well length, the normalized (to one) sum of the ten normalized geologic factors examined. In the case of both well 1 and well 2 a high composite score is associated with the known production intervals (blue sections of the dashed open intervals). This is also the case with all twelve production wells.

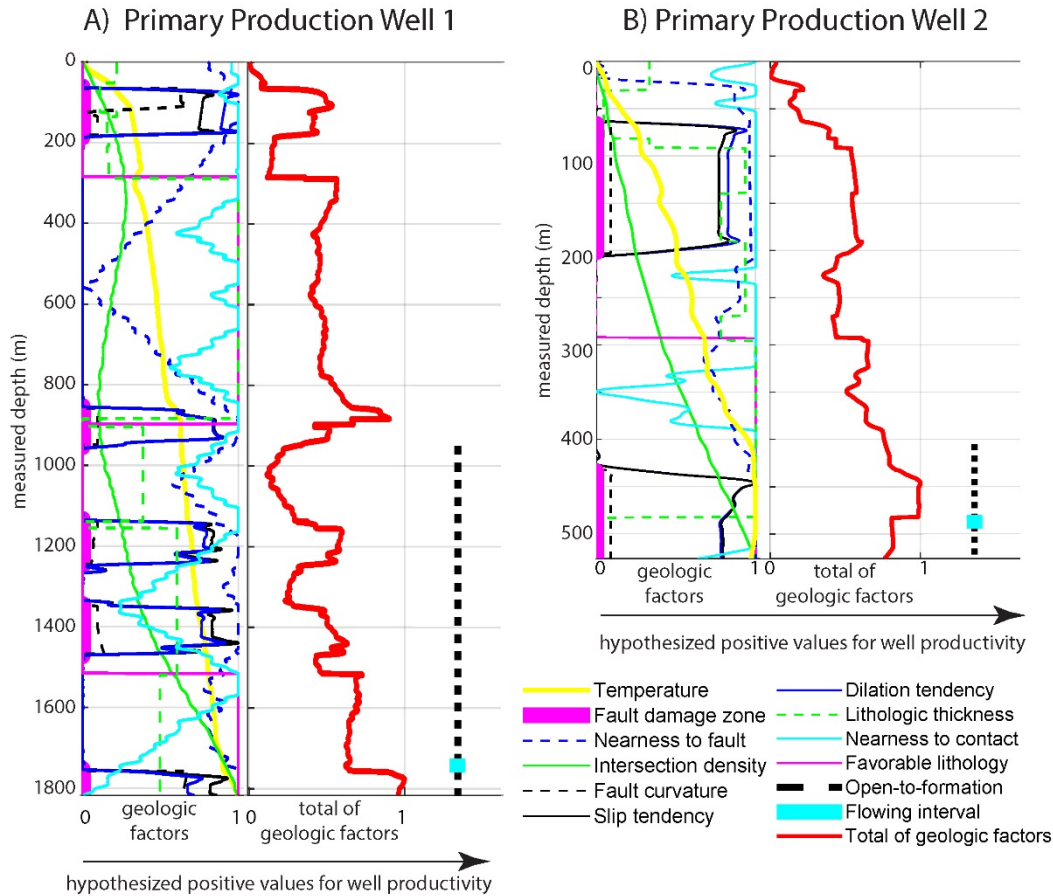


Figure 3. Examples of the geologic factors along two of the primary production wells at Brady. For these two examples, flowing intervals occur where all of the factors are high, giving a composite value ~1.

Figures 4 and 5 show plots of the geologic factors (two different factors for each plot) examined for each of the fifty geothermal wells used in the study. The production wells (small red dots), injection wells (blue dots), non-productive well (green dots), and randomly distributed synthetic wells (very small black dots) are plotted with the same color codes on each plot. Also plotted are the open-to-flow sections of the twelve production wells (open red circles), and the open-to-flow sections of the five primary production wells (large red circles). In Figures 4 and 5 the axes are not labeled with numeric values, but with words indicating relative change in each factor along the axes. See the Methods section for details about how each factor is quantified. Separation along the axes between red and/or blue wells relative to the green wells suggests that the plotted metric has some predictive skill in identifying production or injection wells vs. non-productive wells.

The black arrows along each axis point in the direction hypothesized to result in higher productivity, allowing a rapid assessment of whether or not the data support the conceptual model. For example, on Figures 4A, 4B, and 4C productive wells are expected to plot up and to the right; on 4D productive wells are expected to plot down and to the left.

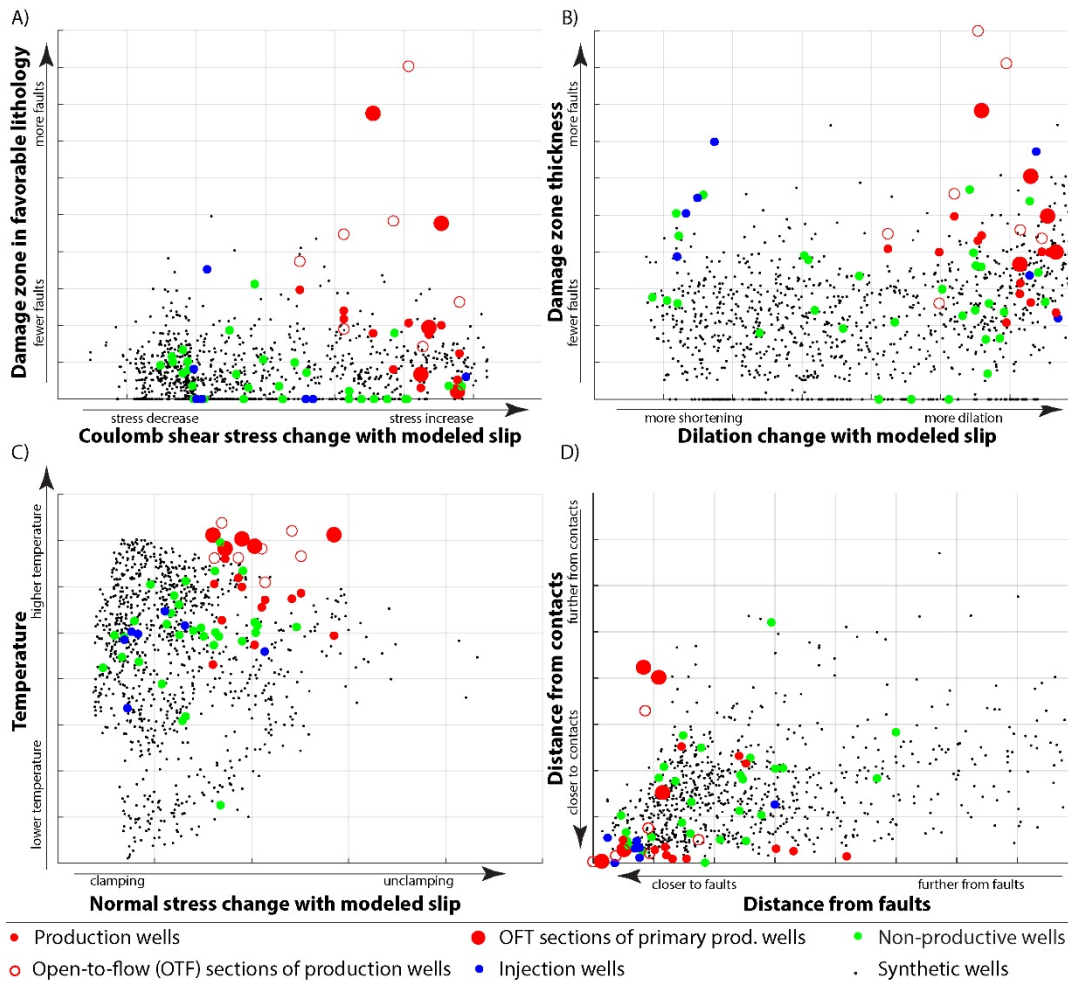


Figure 4. Binary plots of geologic factors. Arrows indicate where production wells are expected to plot relative to non-productive wells for the hypothesized affect of each geologic factor.

Table 1 shows the results of visual inspection of the Figure 4 and Figure 5 plots, indicating whether each geologic factor can be used to distinguish 1) production wells from the randomly distributed synthetic wells; and 2) production wells from non-productive wells. Red highlighted values indicate the factor appears to correlate with relative well productivity as hypothesized. High heat, high damage zone thickness, low distance from faults, high dilation as a result of modeled slip, high reduction in normal stress as a result of modeled slip, increase in Coulomb shear stress as a result of modeled slip, high thickness of fault damage zone in favorable lithologies, and a low distance to geologic contacts all occur along production wells relative to non-productive wells. Fault intersection density may be higher along production wells relative to the synthetic well data set, but the plot is somewhat ambiguous based on initial visual inspection. Thicker stratigraphic units also appear to be marginally more associated with production wells relative to non-productive wells, though again the plot is ambiguous. Fault curvature, slip tendency, and dilation tendency do not appear to be higher along production wells relative to non-productive wells. There appears to be little correlation in the geologic factors along injection wells relative to the non-productive or randomly distributed wells.

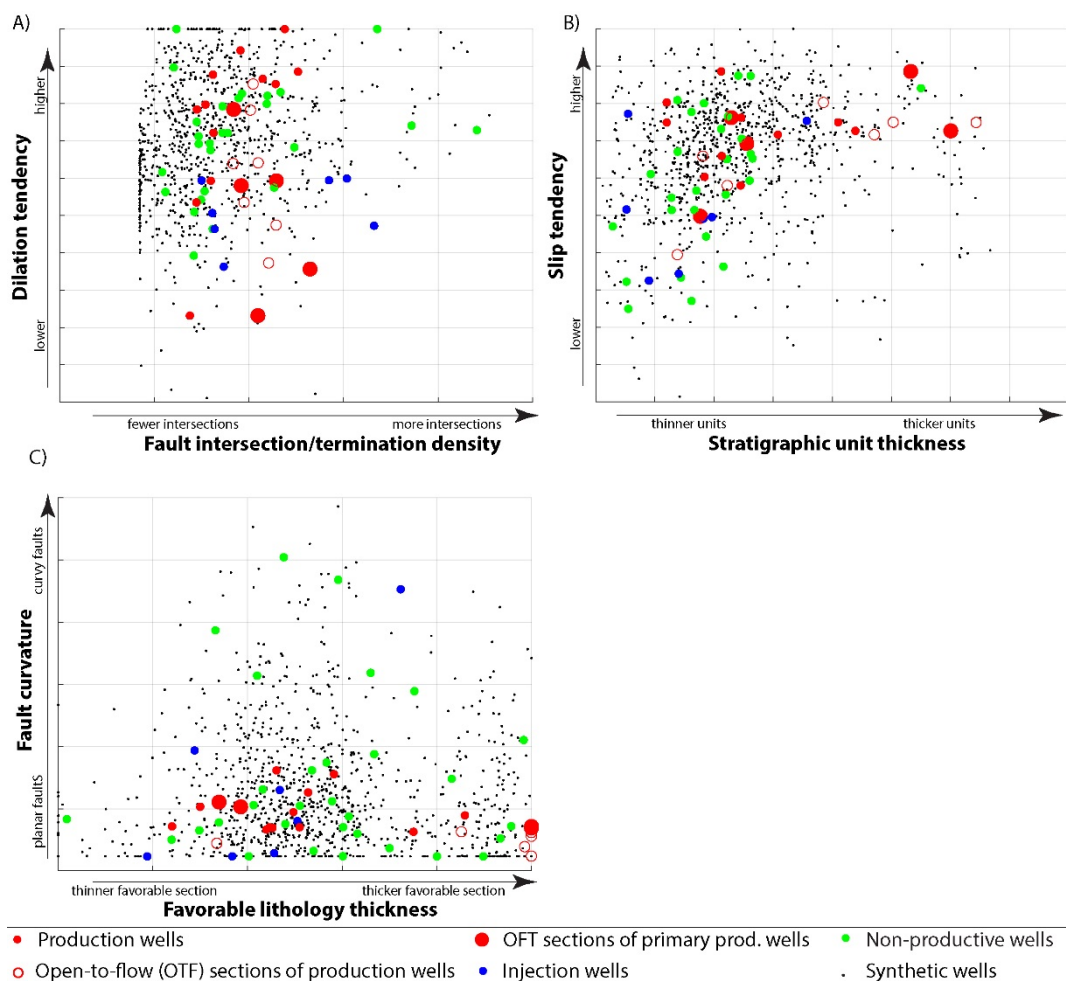


Figure 5. Binary plots of geologic factors. Arrows indicate where production wells are expected to plot relative to non-productive wells for the hypothesized affect of each geologic factor.

5. Discussion

Visual inspection of Figures 4 and 5 indicates that at least eight of the fourteen geologic factors examined occur in higher values or in higher abundance along productive wells relative to the randomly distributed synthetic wells, or the non-productive wells (Table 1). These eight factors are heat, damage zone thickness, distance from faults, dilation as a result of modeled slip, normal stress reduction as a result of modeled slip, Coulomb shear stress increase as a result of modeled slip, damage zone thickness in favorable lithology, and distance from geologic contacts. This suggests 1) wells that encounter these geologic conditions are more likely to be productive than they are to be non-productive, and 2) these eight geologic factors probably play a role in controlling permeability, the connectivity of the fracture system, and ultimately fluid flow to the production wells.

In cases in which production wells fall on the margin of or outside of the ‘background’ geologic conditions, which is denoted by the cloud of the randomly distributed synthetic wells, we suggest that these wells encounter anomalous conditions that may be related to their productivity. For

instance, on Figure 4A the open-to-flow sections of at least six production and primary production wells fall outside of the cloud of synthetic wells. These wells apparently encounter an atypical thickness of faults in favorable lithologies. This characteristic may partially be responsible for their productivity.

In cases where the population of production wells are separated along the axes from the non-productive wells, we suggest that those particular metric(s) may be necessary for production grade fluid flow. For instance, on Figures 4B and 4C the population of production wells appear to have distinctly higher dilation, damage zone thickness, temperature, and normal stress relative to the non-productive wells. These metrics may correlate with production grade fluid flow, and therefore be useful in citing other well locations.

Table 1. Summary of the results of visual inspection of Figures 4 and 5.

	Which plot?	Production wells different from geologic background?	Production wells different from non-productive wells?
Heat	4C y-axis	Higher along production	Higher along production
Damage zone thickness	4B y-axis	Higher along production	Higher along production
Distance from faults	4D x-axis	Lower along production	Lower along production
Fault intersection/ termination density	5A x-axis	No clear correlation	No clear correlation
Fault curvature	5C y-axis	No clear correlation	No clear correlation
Slip tendency	5B y-axis	No clear correlation	No clear correlation
Dilation tendency	5A y-axis	No clear correlation	No clear correlation
Dilation as a result of slip	4B x-axis	Higher along production	Higher along production
Normal stress change as a result of slip	4C x-axis	Higher along production	Higher along production
Coulomb shear stress change as a result of slip	4A x-axis	Higher along production	Higher along production
Thickness of favorable lithologies	5C x-axis	No clear correlation	No clear correlation
Damage zone thickness in favorable lithologies	4A y-axis	Higher along production	Higher along production
Distance from geologic contacts	4D y-axis	Lower along production	Lower along production
Thickness of individual stratigraphic units	5A x-axis	Marginally higher (?) along production	Marginally higher (?) along production

There appears to be no significant correlation between the geologic factors along injection wells relative to the non-productive or randomly distributed wells, or strangely, the production wells. There are several possible explanations for this. Firstly, only seven injection wells are examined in this study, and six of the seven injection wells are between ~150 m and 230 m deep.

Additionally, four of the six injection wells are situated within a very small area, ~500 m of strike length by <25 m across strike length. This means that the injection wells sample a much smaller geologic volume relative to the production wells or non-productive wells, both of which have a much greater range in depth and are more widely distributed. It is possible that this relatively small sample size is insufficient to differentiate the injection wells from the production and non-productive wells. Alternatively, it may be that the porosity and connectivity in the six shallow injection wells is largely controlled by a geologic factor that was not examined in this study, like very high matrix porosity in the shallow stratigraphic section, for instance.

Fault curvature, slip tendency, dilation tendency, intersection/termination density, the thickness of individual stratigraphic units, and the total thickness of favorable lithologic units all appear to be only marginally correlated, or not at all correlated with production wells relative to the non-productive wells and the randomly distributed synthetic wells. It is possible that these geologic factors exert no control on fracture connectivity, upwelling, or fluid flow to the production wells. However, in the cases of fault curvature, slip tendency, and dilation tendency, the maximum value along each well path was used. In essence, we only compared the highest slip tendency fault, dilation tendency fault, and most highly curved fault along each well, with the expectation that the most well oriented and/or curved faults might control the productivity of a well. It is possible that it is not valid to compare these maximum values to the values of other factors, which are integrated along the entire well path.

Alternatively, fault curvature, slip tendency, dilation tendency, intersection/termination density, and the total thickness of favorable lithologic units may be dependent on other factors, like the occurrence or density of faults, to play a role in controlling permeability. Future work will involve principle component analysis in order to examine which factors, and importantly which combinations of factors are most closely correlated with productive wells, and most closely correlated with the discrete productive zones of production wells.

6. Conclusions

Fifty wells in the Brady geothermal field were examined using fourteen geologic factors to address the question posed in the title: Can geologic factors be predictive for distinguishing between productive and non-productive geothermal wells? The geologic factors used in this study are constrained by a detailed 3D geologic map of the Brady geothermal area, a published 3D stress model, and by published numerical modeling of the stress and strain effects of local fault slip. Results indicate that at least eight of the geologic factors examined in the study appear to have predictive skill for distinguishing productive wells from non-productive wells. These eight factors are heat, damage zone thickness, distance from faults, dilation associated with modeled fault slip, normal stress change associated with modeled fault slip, Coulomb shear stress change associated with modeled fault slip, fault damage zone thickness in favorable lithologies, and nearness to geologic contacts. Based on the biplots, fault intersection/termination density, slip tendency, dilation tendency, fault curvature, and thickness of favorable lithologies do not appear to be predictive for differentiating productive from non-productive wells. These factors may exert only minor influence on fracture connectivity and fluid flow, but future multivariate analyses are needed to evaluate the complex interrelationships between all factors. At least eight of the factors examined herein, which are related to the distribution and geometry

of faults, the geometry of the stratigraphic section, the ambient stress conditions, and the distribution of heat in the subsurface are correlated with production wells. We infer that these factors play an important role the development and maintenance of the large, interconnected fracture systems that conduct geothermal fluid circulation in this geothermal field, and perhaps other fields as well.

Acknowledgments

The 3D geologic map of the Brady system was supported by Ormat and the U.S. Department of Energy under award DE-FG36-08GO18200 and DE-FG36-02ID14311 to Ormat Technologies, Inc. Funds associated with Geothermal Resources Investigations Project at the U.S. Geologic Survey supported this project. Any use of trade, firm, or product names is for descriptive purposes only and does not imply endorsement by the U.S. Government.

REFERENCES

- Ali, S.T., Akerley, J., Baluyut, E.C., Cardiff, M., Davatzes, N.C., Feigl, K.L., Foxall, W., Fratta, D., Mellors, R.J., Spielman, P., and others, 2016, Time-series analysis of surface deformation at Brady Hot Springs geothermal field (Nevada) using interferometric synthetic aperture radar: *Geothermics*, v. 61, p. 114–120.
- Barton, C.A., Zoback, M.D., and Moos, D., 1995, Fluid flow along potentially active faults in crystalline rock: *Geology*, v. 23, no. 8, p. 23–27, doi: 10.1130/0091-7613(1995)023<0683.
- Cowie, P.A., and Scholz, C.H., 1992, Displacement-length scaling relationship for faults: data synthesis and discussion: *Journal of Structural Geology*, v. 14, no. 10, p. 1149–1156.
- Faulds, J.E., Coolbaugh, M.F., Benoit, W.R., Oppliger, G.L., Perkins, M., Moeck, I., and Drakos, P.S., 2010a, Structural Controls of Geothermal Activity in the Northern Hot Springs Mountains, Western Nevada: The Tale of Three Geothermal Systems (Brady's, Desert Peak, and Desert Queen): *Geothermal Resources Council Transactions*, v. 34, p. 675–684.
- Faulds, J.E., Moeck, I., Drakos, P.S., and Zemach, E., 2010b, Structural Assessment and 3D geologic modeling of the Brady's geothermal area, Churchill County (Nevada, USA): A preliminary report, *in* Proceedings, Thirty-Fifth Workshop on Geothermal Reservoir Engineering, Stanford University, p. 298–302.
- Faulds, J.E., Ramelli, A.R., Coolbaugh, M.F., Hinz, N.H., Garside, L.J., and Queen, J.H., 2017, Preliminary Geologic Map of the Bradys Geothermal Area, Churchill County, Nevada: Nevada Bureau of Mines and Geology, Open-File Report 17-4, scale 1:12,000.
- Fossen, H., and Rotevatn, A., 2016, Fault linkage and relay structures in extensional settings—A review: *Earth-Science Reviews*, v. 154, p. 14–28.
- Jolie, E., Faulds, J.E., and Moeck, I., 2012, The Development of a 3D structural-geological model as part of the geothermal exploration strategy - A case study from the Brady's

- geothermal system, Nevada, USA, *in* Proceedings, Thirty-Seventh Workshop on Geothermal Reservoir Engineering, Stanford University, p. 421–425.
- Jolie, E., Moeck, I., and Faulds, J.E., 2015, Quantitative structural–geological exploration of fault-controlled geothermal systems—A case study from the Basin-and-Range Province, Nevada (USA): *Geothermics*, v. 54, p. 54–67, doi: 10.1016/j.geothermics.2014.10.003.
- Kratt, C., Calvin, W., and Coolbaugh, M.F., 2006, Geothermal exploration with Hymap hyperspectral data at Brady–Desert Peak, Nevada: *Remote Sensing of Environment*, v. 104, no. 3, p. 313–324, doi: 10.1016/j.rse.2006.05.005.
- Lechler, P.J., and Coolbaugh, M.F., 2007, Gaseous Emissions from Steamboat Springs, Brady’s Hot Springs, and Desert Peak Geothermal Systems, Nevada: *Geothermal Resources Council Transactions*, v. 31, p. 359–361.
- Moeck, I., Kwiatek, G., and Zimmerman, G., 2009a, Slip tendency analysis , fault reactivation potential and induced seismicity in a deep geothermal reservoir: *Journal of Structural Geology*, v. 31, p. 1174–1182, doi: 10.1016/j.jsg.2009.06.012.
- Moeck, I., Schandelmeier, Æ.H., and Holl, H., 2009b, The stress regime in a Rotliegend reservoir of the Northeast German Basin: *International Journal of Earth Sciences*, v. 98, p. 1643–1654, doi: 10.1007/s00531-008-0316-1.
- Morris, A., Ferrill, D.A., and Henderson, D.B., 1996, Slip-tendency analysis and fault reactivation: *Geology*, v. 24, no. 3, p. 275–278.
- Peacock, D.C.P., Knipe, R.J., and Sanderson, D.J., 2000, Glossary of normal faults: *Journal of Structural Geology*, v. 22, p. 291–305.
- Pollard, D.D., and Aydin, A., 1988, Progress in understanding jointing over the past century Progress in understanding jointing over the past century: *Geological Society of America Bulletin*, v. 100, no. 8, p. 1181–1204, doi: 10.1130/0016-7606(1988)100<1181.
- Queen, J.H., Daley, T.M., Majer, E.L., Nihei, K.T., Siler, D.L., and Faulds, J.E., 2016, Surface Reflection Seismic and Vertical Seismic Profile at Brady’s Hot Springs, NV, USA, *in* Proceedings, Forty-First Workshop on Geothermal Reservoir Engineering, Stanford University, p. 14.
- Rubin, A.M., and Pollard, D.D., 1988, Geology Dike-induced faulting in rift zones of Iceland and Afar Dike-induced faulting in rift zones of Iceland and Afar: *Geology*, v. 16, p. 413–417, doi: 10.1130/0091-7613(1988)016<0413.
- Sanderson, D.J., and Zhang, X., 2004, Stress-controlled localization of deformation and fluid flow in fractured rocks: *Geological Society, London, Special Publications*, v. 231, no. 1, p. 299–314.
- Scholz, C.H., Dawers, N.H., Yu, J., Anders, M.H., and Cowie, P.A., 1993, Fault Growth and Fault Scaling Laws: Preliminary Results: *Journal of Geophysical Research*, v. 98, no. B12, p. 951–961.
- Shevenell, L.A., Oppliger, G., Coolbaugh, M.F., and Faulds, J.E., 2012, Bradys (Nevada) InSAR Anomaly Evaluated With Historical Well Temperature and Pressure Data: *Geothermal Resources Council Transactions*, v. 36, p. 1383–1390.

- Sibson, R.H., 1994, Crustal stress, faulting and fluid flow, *in* Parnell, J. ed., *Geofluids: Origin, Migration and Evolution of Fluids in Sedimentary Basins*, Geological Society, London, Special Publications, p. 69–84.
- Siler, D.L., and Faulds, J.E., 2013, Three-dimensional geothermal fairway mapping: Examples from the western Great Basin, USA, *in* *Geothermal Resources Council Transactions*,.
- Siler, D.L., Faulds, J.E., and Hinz, N.H., 2015, Earthquake-related stress concentrations and permeability generation in geothermal systems, *in* *Geothermal Resources Council Transactions*,.
- Siler, D.L., Faulds, J.E., Hinz, N.H., Dering, G.M., Edwards, J.H., and Mayhew, B., 2019, Three-dimensional geologic mapping to assess geothermal potential: examples from Nevada and Oregon: *Geothermal Energy*, v. 7, no. 1, p. 2, doi: 10.1186/s40517-018-0117-0.
- Siler, D.L., Hinz, N.H., and Faulds, J.E., 2018, Stress concentrations at structural discontinuities in active fault zones in the western United States: Implications for permeability and fluid flow in geothermal fields: *Geological Society of America Bulletin*, doi: <https://doi.org/10.1130/B31729.1>.
- Siler, D.L., Hinz, N.H., Faulds, J.E., and Queen, J., 2016, 3D Analysis of Geothermal Fluid Flow Favorability: Brady's, Nevada, USA: The 41st Workshop on Geothermal Reservoir Engineering, Stanford University, v. 41, p. 10.
- Wesnousky, S.G., Barron, A.D., Briggs, R.W., Caskey, S.J., Kumar, S., and Owen, L., 2005, Paleoseismic transect across the northern Great Basin: *Journal of Geophysical Research B: Solid Earth*, v. 110, no. 5, p. 1–25, doi: 10.1029/2004JB003283.
- Witter, J.B., Siler, D.L., Faulds, J.E., and Hinz, N.H., 2016, 3D geophysical inversion modeling of gravity data to test the 3D geologic model of the Bradys geothermal area, Nevada, USA: *Geothermal Energy*, v. 4, no. 14, p. 21, doi: 10.1186/s40517-016-0056-6.
- Zoback, M.D., and Townend, J., 2001, Implications of hydrostatic pore pressures and high crustal strength for the deformation of intraplate lithosphere: *Tectonophysics*, v. 336, no. 1–4, p. 19–30, doi: 10.1016/S0040-1951(01)00091-9.